Available online at www.sciencedirect.com
ScienceDirect
Trans. Nonferrous Met. Soc. China 31(2021) 2664−2676
Transactions of Nonferrous Metals Society of China
www.tnmsc.cn

Static globularization and grain morphology evolution of α and β phases during annealing of hot-rolled TC21 titanium alloy

Ke WANG, Ming-yu WU, Zhao REN, Yu ZHANG, Ren-long XIN, Qing LIU

International Joint Laboratory for Light Alloys (MOE),
College of Materials Science and Engineering, Chongqing University, Chongqing 400044, China

Received 30 September 2020; accepted 7 April 2021

Abstract: A lamellar-structure TC21 titanium alloy was hot-rolled and subsequently annealed at 820, 880 and 940 °C for 1 and 6 h, and the effects of annealing parameters on static globularization and morphology evolution of both α and β phases were studied. The results show that α globularization process is sluggish due to the limited boundary splitting at 820 °C. With increasing temperature to 880 °C, the accelerated boundary splitting and termination migration promote the α globularization. At 820 and 880 °C, the static recovery (SRV) and recrystallization (SRX) induce the grain refinement of interlamellar β phase. However, the excessively high temperature of 940 °C results in the coarsening of α grains due to the assistance of Ostwald ripening, and produces coarse β grains mainly due to the absence of SRX in interlamellar β phases. Conclusively, 880 °C is an appropriate annealing temperature to produce a homogeneous microstructure in which globularized α and refined β grains distribute homogeneously.
Key words: TC21 titanium alloy; α globularization; recrystallization; grain refinement

1 Introduction

The α/β titanium alloys are widely used in aerospace, biomedical, and chemical industries owing to their excellent mechanical and physical properties, outstanding corrosion and oxidation resistance, good creep resistance, etc [1−4]. Lamellar structure is a typical microstructure of titanium alloy, in which the lamellar α is always formed as many colonies within the former β grains. This microstructure can be simply developed during cooling from high temperature in the single-phase β field, and the thickness of α lamellae closely depends on the cooling rate. Since lamellar structure does not possess a good balance between strength and ductility, titanium alloys with equiaxed or bimodal structures are more desirable, in which a part of α phases exist as an equiaxed morphology [5].

The lamellar structure in titanium alloys cannot evolve into an equiaxed structure via only annealing treatment. This is because the anisotropy of α/β interfacial energy leads to selective growth of α phase in certain orientations [6]. Generally, hot deformation should be carried out on the lamellar-structure titanium alloys before heat treatment, and it could induce dynamic globularization during deformation [7−9]. The dynamic globularization fraction of α phase increases with increasing strain and temperature, but decreases with increasing strain rate [10]. However, full globularization is generally difficult to be achieved by hot deformation [11,12]. The assistance of static globularization during subsequent heat treatment is essential to achieve the full globularization of lamellar α.

Thus far, several mechanisms have been proposed to interpret the static globularization process, and the boundary splitting and termination

Corresponding author: Ke WANG, Tel: +86-18502348389, E-mail: study_ke@cqu.edu.cn
DOI: 10.1016/S1003-6326(21)65683-2

migration are the two dominant mechanisms for the static globularization during heat treatment [13−15]. Boundary splitting was generally considered to occur during the initial stages of static spheroidization [16], in which β phase penetrated through α lamellae along boundaries generated via recovery and recrystallization. During prolonged annealing time [17], the termination migration played a key role in static globularization and grain coarsening. Meanwhile, Ostwald ripening was also found to influence the microstructure coarsening and globularization [18,19]. Based on the analysis about globularization mechanism, globularization kinetics was well interpreted [20,21]. Additionally, the heterogeneous deformation due to different crystallographic orientations of α colonies could cause heterogeneous static globularization during subsequent annealing [22]. ROY et al [23−25] suggested that the static globularization process of individual α colony is related to the crystallographic orientation with respect to the straining direction.

Although a large number of studies have been performed on the mechanism and kinetics of globularization of lamellar α, the combined effect of annealing temperature and annealing time on α globularization needs some fundamental investigations. Moreover, the globularization and distribution of α grains also depend on β phase evolution during annealing, which also lacks sufficient study. To clarify the globularization process of α phase, electron backscatter diffraction (EBSD) was performed on the TC21 titanium alloy subjected to hot rolling and subsequent annealing with different temperatures and time. The results obtained in this study could provide a guidance for controlling the microstructure and optimizing the properties of TC21 and other titanium alloys.

2 Experimental

2.1 Materials

The as-received TC21 titanium alloy was a forged rod with diameter of 400 mm. Its chemical composition (in wt.%) was 6.28 Al, 3.06 Mo, 1.89 Nb, 2.04 Sn, 2.18 Zr, 1.61 Cr, 0.066 Si, 0.022 Fe, 0.009 C, 0.122 O, 0.005 N, and balance Ti. The β transus temperature was approximately 960 °C for this alloy.

The total experimental process in this study is schematically illustrated in Fig. 1. The rectangular samples with dimensions of 30 mm (TD) × 6 mm (ND) × 20 mm (RD) were machined from the as-received rod. Here, RD, TD and ND refer to the rolling direction, transverse direction and normal direction, respectively. The RD is parallel to the longitudinal direction of the as-received rod. Before hot rolling, the rectangular samples were held at 1000 °C for 1 h and followed by furnace cooling to develop a lamellar microstructure, as shown in Fig. 2. Additionally, the (0001) plane and one of $\langle 11\bar{2}0\rangle$ directions of the lamellar α are nearly parallel to one of the {110} planes and one of the $\langle 111\rangle$ directions of the neighboring interlamellar β (Fig. 2(d)), indicating that the lamellar α and interlamellar β in one colony keep the Burgers orientation relationship (OR), i.e. $(0001)_\alpha // \{110\}_\beta$ and $\langle 11\bar{2}0\rangle_\alpha // \langle 111\rangle_\beta$ [26].

2.2 Hot rolling and annealing

The rectangular specimens were hot-rolled with a total height reduction of 60% through a four-pass process at 750 °C. The reduction per rolling pass was imposed to ~15%. During every rolling pass, the specimen was reheated at 750 °C

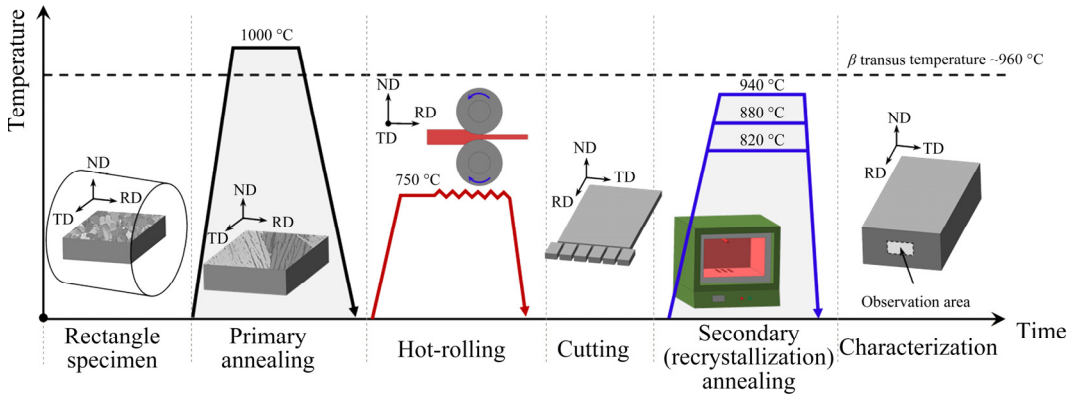

Fig. 1 Schematic illustration of specimen preparation and characterization for rolled and annealed specimens

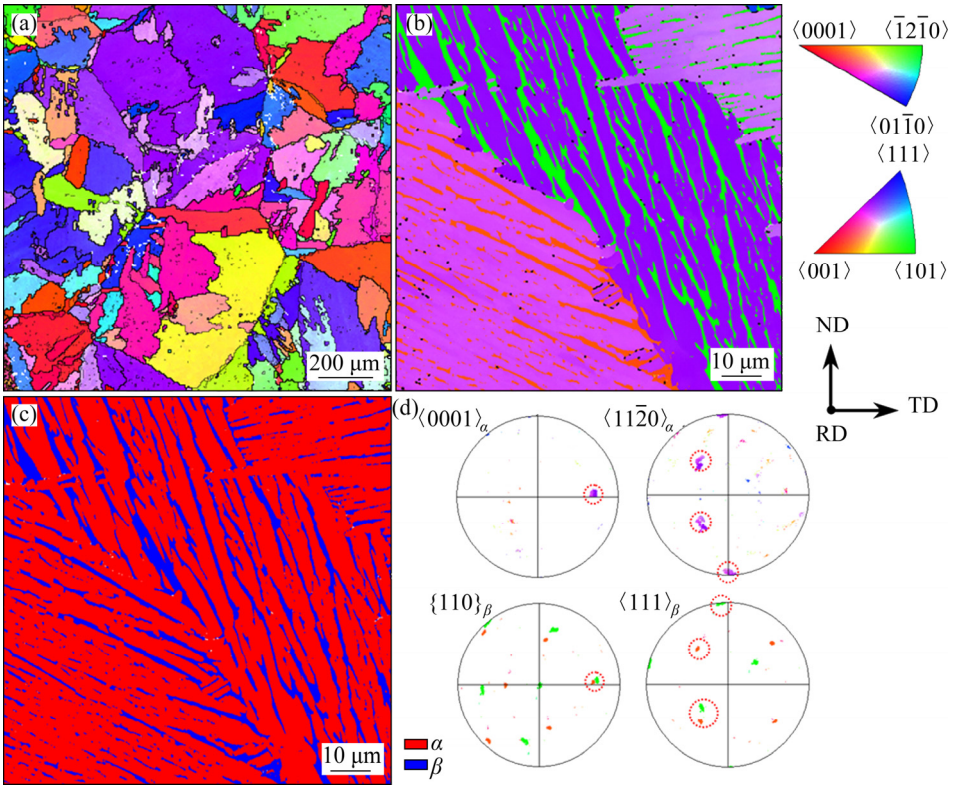

Fig. 2 Non-rolled microstructures of TC21 titanium alloy held at 1000 °C for 1 h followed by furnace cooling: (a) Low-magnification inverse pole figure (IPF) map; (b) High-magnification IPF map; (c) Phase map corresponding to (b); (d) Pole figures of α and β phases corresponding to (b) (The poles marked by circles in (d) indicate the parallel crystallographic planes and directions)

for 5 min. Finally, the specimen was air-cooled after the final pass. After the rolling, smaller samples of 4 mm (TD) × 2.4 mm (ND) × 8 mm (RD) were prepared from the hot-rolled plates for annealing at 820, 880 and 940 °C for 1 and 6 h, respectively. After annealing, the specimens were cooled in air to room temperature.

2.3 Microstructure observation

The microstructure observation was performed on the cross sectional ND−TD plane at the mid-thickness regions of the non-rolled, rolled and annealed samples. The specimens for EBSD were mechanically ground and then electro-polished in a solution of 60% methanol, 34% n-butyl alcohol and 6% perchloric acid at room temperature and 17 V using an electric polishing machine (Struers LectroPol-5). EBSD characterization was performed using a Tescan MIRA3 field emission gun scanning electron microscope (SEM) operated at 20 kV and equipped with an EBSD detector. EBSD data were collected by Oxford AZtec acquisition software package. During EBSD experiment, the sample surface was tilted by 70° with respect to EBSD detector. The scanning step size was set to be 0.15−0.7 μm according to grain size of the samples. The offline data analysis was carried out using HKL Technology Channel 5 software. Meanwhile, a Tecnai F20 G^2 TEM was also employed to characterize the microstructure, in which the characterized slice sectioned from the hot-rolled specimen was ground to 50−70 μm followed by twin-jet electropolishing.

3 Results and discussion

3.1 Hot-rolled microstructure

The microstructure evolution of α/β titanium alloy during hot deformation is largely determined by deformation temperature. Generally, a high rolling temperature could generate dynamic globularization feature in the (α+β) region [27]. The IPF maps of hot-rolled TC21 titanium alloy are shown in Figs. 3(a, b). Within the hot-rolled microstructure, most of α colonies still remain a

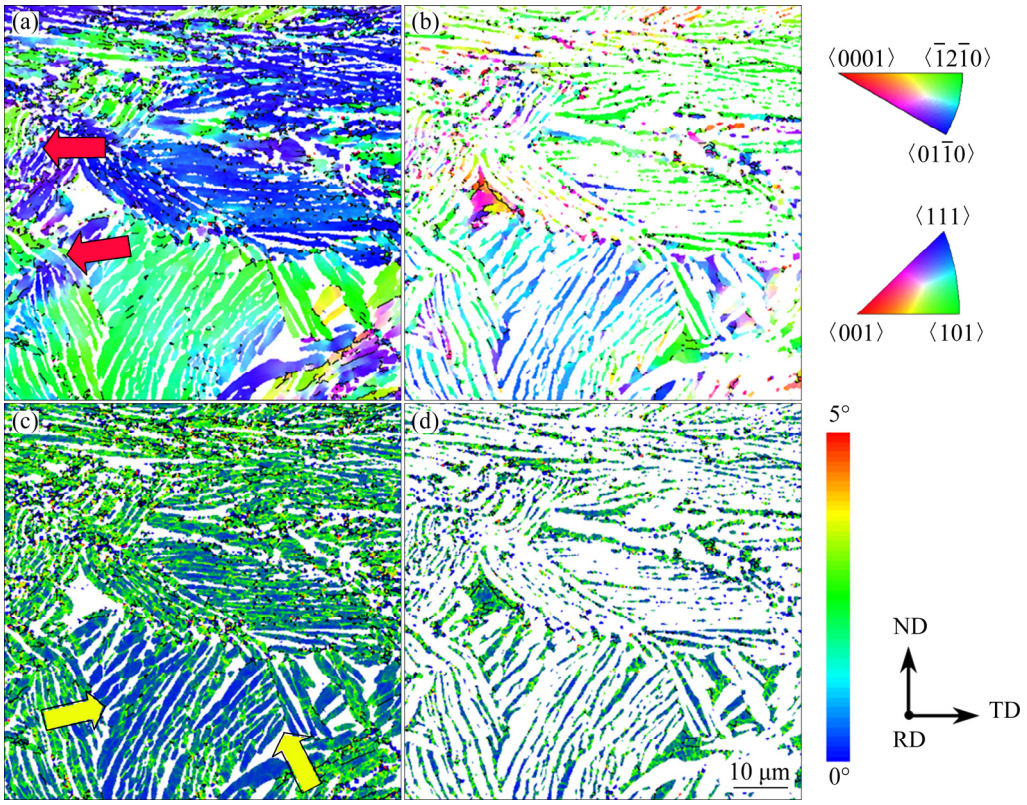

Fig. 3 IPF maps (a, b) and KAM maps (c, d) showing morphology, orientation and local misorientation of α and β phases in hot-rolled TC21 titanium alloy: (a, c) α phase; (b, d) β phase

straight morphology, and only a few α colonies are kinked, as pointed out by the red arrows in Fig. 3(a). Furthermore, the TEM micrograph (Fig. 4) shows that a large amount of dislocation generates in the lamellar α and interlamellar β phases, and few low angle boundaries (LAGBs) and high angle boundaries (HAGBs) exist in them. This phenomenon indicates that the low rolling temperature of 750 °C suppresses the occurrence of dynamic globularization, dynamic recovery (DRV) and dynamic recrystallization (DRX), which will highlight the effect of annealing parameters on the static globularization behavior.

The variation of crystallographic orientation in different colonies could arouse deformation heterogeneity, which subsequently leads to heterogeneous distribution of the geometric morphology and dislocation density among these colonies. The formation of kinked α colony can be attributed to 'hard' orientation [25,28]. Kernel average misorientation (KAM) map has been widely used to indicate the relative content of geometric necessary dislocations [29]. As shown in the KAM maps (Figs. 3(c, d)), although most of α

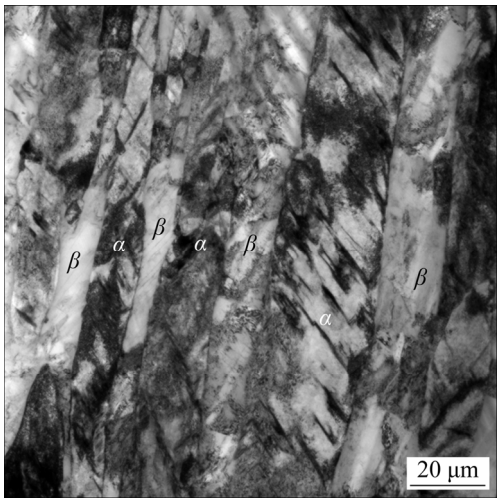

Fig. 4 Typical TEM micrograph of hot-rolled TC21 titanium alloy

colonies possess high dislocation density, some lamellar α phases, as pointed out by the yellow arrows in Figs. 3(c, d), have relatively low dislocation density. Apparently, the higher dislocation density suggests a larger deformation amount due to the 'soft' orientation of the lamellar α.

3.2 Microstructure evolution at 820 °C

The typical microstructure evolution at the annealing temperature of 820 °C can be clearly reflected by phase maps and IPF maps, as shown in Fig. 5. When annealed at 820 °C for 1 h, many LAGBs and HAGBs are formed by SRV and SRX in the α lamellae. However, most of the colonies maintain the integrated-lamellar morphology except for a few bent and kinked lamellae (as pointed by black color in Fig. 5(c)). This microstructure is similar with that of the hot-rolled TC21 titanium alloy, indicating that no apparent globularization occurs. With increasing annealing time to 6 h, more LAGBs and HAGBs appearing in the α lamellae suggest an enhancement of SRV and SRX. In addition, a heterogeneous SRX feature exists in

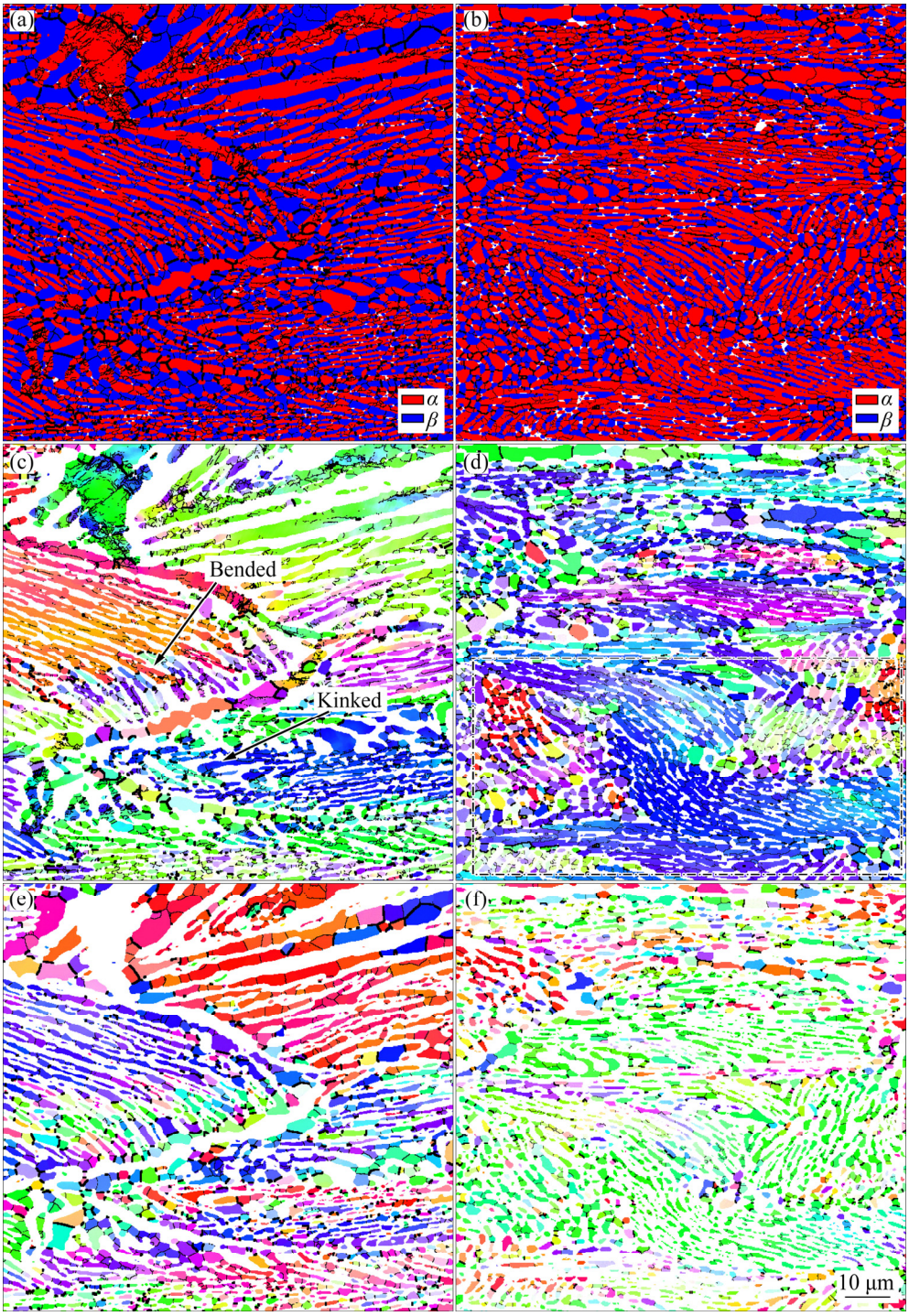

Fig. 5 Phase maps (a, b) and IPF maps of separated α (c, d) and β (e, f) phases in annealed microstructures acquired by annealing at 820 °C for different time: (a, c, e) 1 h; (b, d, f) 6 h

different colonies, as pointed out by the rectangular box in Fig. 5(d). The heterogeneous SRX feature can be analyzed by the enlarged IPF map in Fig. 6, in which colonies A and C express a higher content of HAGBs (stronger SRX) in the α lamellae than colonies B and D (Fig. 6(a)). Noticeably, the LAGBs and HAGBs divide the α lamellae into many subgrains and SRXed grains, but these grains are adjacent to each other rather than separated from each other. Such phenomenon indicates that annealing at 820 °C just induces a limited globularization of α lamellae, even with an enhancement of SRX as the annealing time prolongs to 6 h.

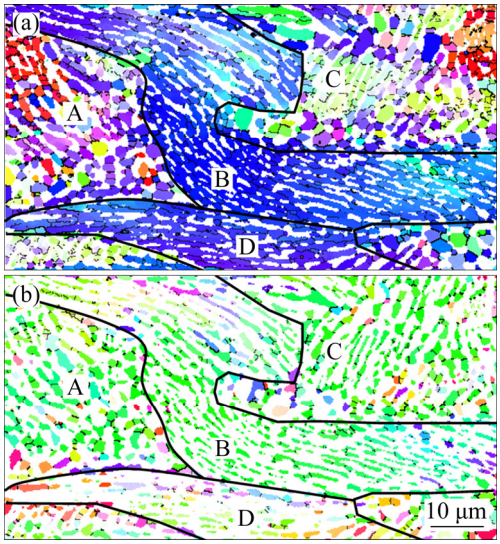

Fig. 6 Heterogeneous SRX feature of α (a) and β (b) phases in annealed microstructure treated by annealing at 820 °C for 6 h

The very sluggish globularization of the α lamellae at 820 °C can be interpreted based on the globularization mechanism. As shown in the local magnified IPF map of Fig. 6(a), the α lamellae show a remarkable-serrated profile that many grooves appear on the interface of α lamellae. This indicates that boundary splitting occurs during annealing. The process of boundary splitting can be illustrated by Fig. 7(a), in which the β phase penetrates through the α lamellae along LAGBs and HAGBs to form the globularized α grains. It is assumed that a low temperature (820 °C) and short annealing time (1 h) not only suppress the formation of LAGBs and HAGBs via SRV and SRX, but also restrain β phase penetration, so that the fraction of globularized α grains is very limited. Even with increasing annealing time to 6 h, the occurrence of SRV and SRX is just enhanced in lamellar α, and the low temperature at 820 °C still restrains β phase penetration, so the α globularization fraction keeps limited.

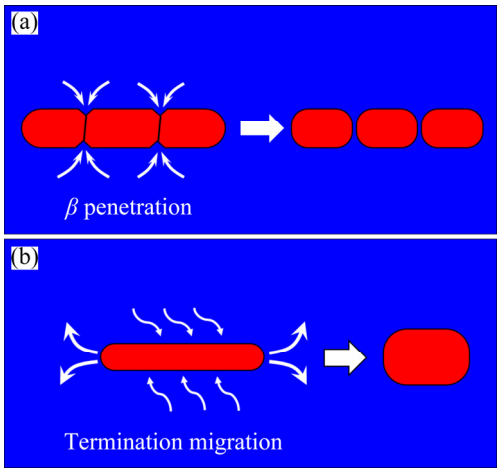

Fig. 7 Schematic illustration of globularization mechanism of boundary splitting (a) and termination migration (b)

In addition, the interlamellar β also undergoes remarkable morphology evolution during annealing at 820 °C (Figs. 5(e, f)). As shown in Fig. 5(e), some LAGBs and HAGBs are formed in β phase during annealing, which divide the interlamellar β into refined and equiaxed grains. Apparently, increasing annealing time significantly enhances the SRV and SRX in β phase, resulting in more refined and equiaxed β grains (Fig. 5(f)).

3.3 Microstructure evolution at 880 °C

When the annealing temperature increases from 820 to 880 °C, more LAGBs and HAGBs appear in the α lamellae, which divide α lamellae into many subgrains and SRXed grains, as shown in Fig. 8. However, most of subgrains and SRXed grains are still adjacent to each other after the annealing for 1 h, indicating a low globularization fraction of α lamellae. Meanwhile, heterogeneous SRV/SRX features are found at 880 °C for 1 h. As shown in Fig. 8(c), Region A keeps a lamellar morphology with few LAGBs and HAGBs. When the annealing time increases to 6 h, the sufficient and homogeneous α globularization is achieved (Fig. 8(d)).

The full α globularization at the annealing condition of 880 °C, 6 h can be firstly attributed to acceleration of boundary splitting; i.e. increasing

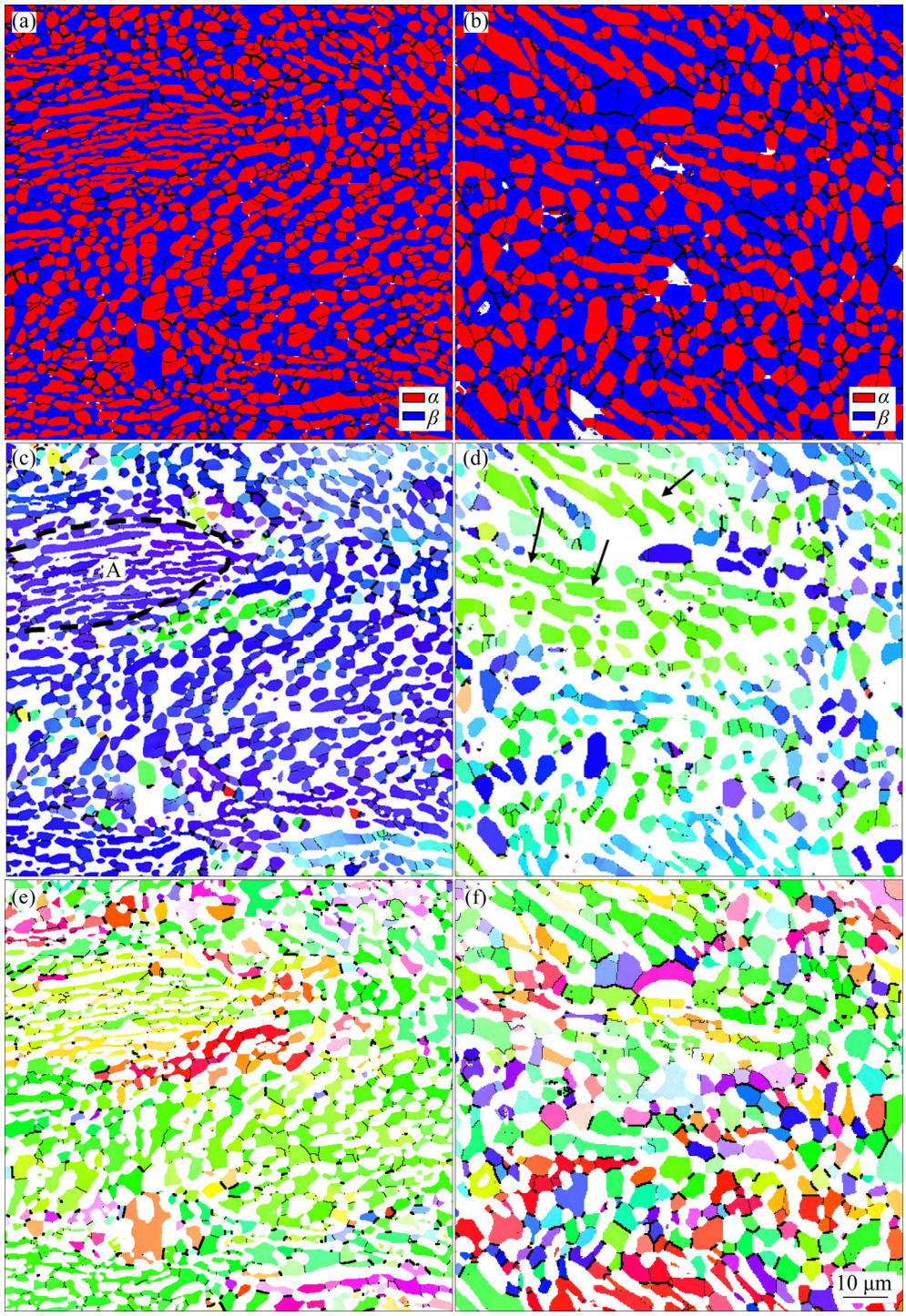

Fig. 8 Phase maps (a, b) and IPF maps of separated α (c, d) and β (e, f) phases in annealed microstructures acquired by annealing at 880 °C for different time: (a, c, e) 1 h; (b, d, f) 6 h

temperature not only promotes the formation of LAGBs and HAGBs, but also enhances β phase penetration through the α lamellae. Secondly, the sufficient α globularization at 880 °C for 6 h could be ascribed to the activation of termination migration. As pointed by black arrows in Fig. 8(d), some α lamellae still possess only a few LAGBs and HAGBs, but these α lamellae become shorter and coarser than the original α lamellae in the rolled microstructure. The above results suggest that termination migration assists and promotes the globularization of α lamellae at 880 °C, 6 h. As shown in the schematic illustration in Fig. 7(b), the process of termination migration includes mass flow of alloy element from termination tips to flat interfaces of α lamellae, resulting in the

dissolution of termination tip and the thickening of α lamellae [18,30]. Therefore, even without formation LAGBs/HAGBs in α lamellae with small deformation amount, the combined effect of high annealing temperature (880 °C) and long annealing time (6 h) significantly promotes the globularization of α lamellae by termination migration.

More homogeneous grain refinement of β phase is found when annealing temperature increases from 820 to 880 °C (Figs. 8(e, f)). Specifically, increasing the annealing temperature significantly enhances SRV and SRX in inter-lamellar β, and thus the increased LAGBs and HAGBs divide the interlamellar β into refined and equiaxed grains. Moreover, it can be seen from Fig. 8(b) that globularized α grains and refined β grains are adjacent to each other and homogeneously distribute in the microstructure.

3.4 Microstructure evolution at 940 °C

As annealing temperature increases largely to 940 °C, the morphology of both α and β phases is significantly different from that at low temperatures of 820 and 880 °C. As shown in Fig. 9, the grain size of α phase at 940 °C is much larger than that of

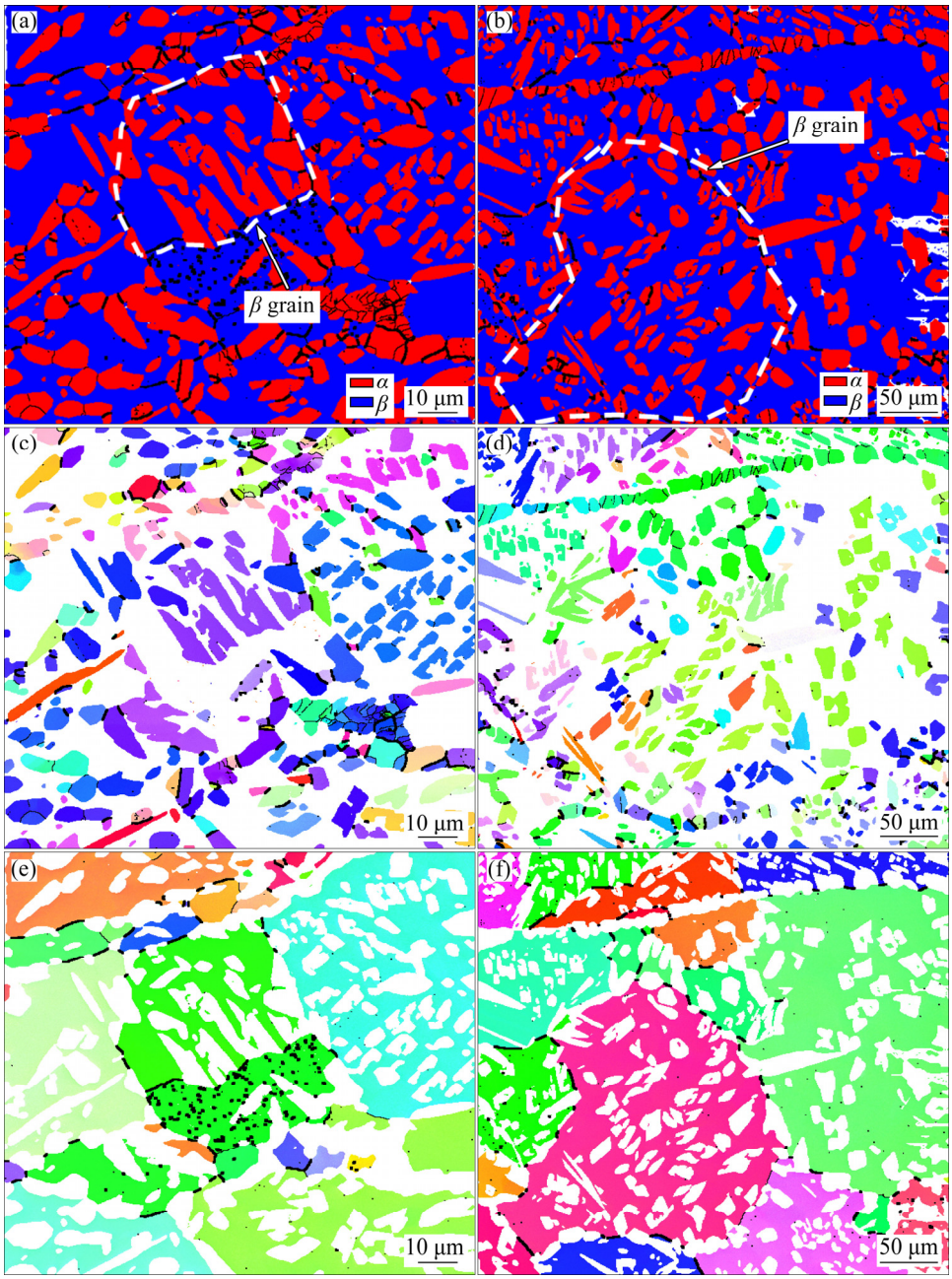

Fig. 9 Phase maps (a, b) and IPF maps of separated α (c, d) and β (e, f) phases in annealed microstructures acquired by annealing at 940 °C for different time: (a, c, e) 1 h; (b, d, f) 6 h

α phase at 820 and 880 °C. Local enlarged IPF maps of α and β phases are shown in Fig. 10. It can be seen that many α grains show an irregular morphology, and only a few α grains express a regular and globularized morphology. Meanwhile, increasing annealing time from 1 h (Fig. 9(a)) to 6 h (Fig. 9(b)) increases the volume fraction of globularized α grains, which can be attributed to the fact that the prolonged annealing time promotes the termination migration to enhance α globularization. The larger α grain size could be attributed to coarsening via Ostwald ripening [29], in which large-sized α particles grow at the expense of small-sized α particles to reduce the total free energy of the system. As reported in the literatures [31−33], Ostwald ripening of α phase involves as α (small-sized particles) → β (matrix) → α (large- sized particles).

Compared with the samples annealed at 820 or 880 °C, refinement of coarse β grains is not observed in the sample annealed at 940 °C. As mentioned in Sections 3.2 and 3.3, when annealed at 820 and 880 °C, LAGBs and HAGBs are formed in β grains via SRV and SRX, which divide interlamellar β into refined grains. Meanwhile, the abundant α grains around β phase generate a strong pinning effect on grain boundary migration of β phase, which effectively restrains β grain growth. In contrast, the coarse β grain would be mainly attributed to the suppressing of SRX at 940 °C. The evolution behavior of SRX can be reflected by EBSD-derived internal average misorientation angle (IAMA) map [34]. In IAMA map, grains with IAMA above 1° are classified as deformed regions (marked by red). If the grains contain subgrains whose IAMA is under 1° but the misorientation from subgrain to subgrain is above 1°, these grains are classified as substructured regions (marked by yellow). All the remaining grains are classified as recrystallized regions (marked by blue). As shown in Fig. 11, IAMA maps clearly show that the fraction of SRX increases as annealing temperature increases from 820 to 880 °C, but decreases sharply from 880 to 940 °C. Thus, the weakened SRX suppresses the generation of HAGBs in inter-lamellar β and induces the coarse β grain at 940 °C. The suppressing of SRX in β phase is possibly related to the $\alpha \rightarrow \beta$ phase transformation at 940 °C. As shown in Fig. 12, the volume fraction of β phase gradually increases with increasing annealing temperature. As a result, the rapid phase transformation at an excessive temperature (940 °C) may consume a large amount of stored strain energy in β grains to suppress the SRX. Meanwhile, the formation of LAGB needs enough dislocations [35]. Therefore, the low stored strain energy, resulting

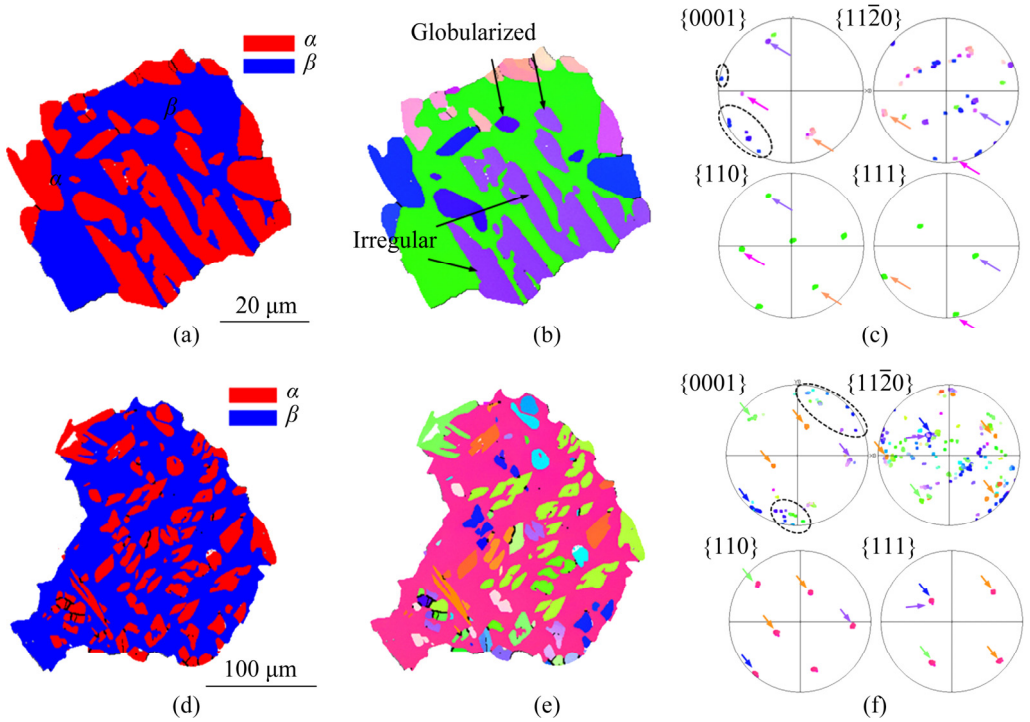

Fig. 10 Orientation relationship between α and β phases in annealed microstructures acquired by annealing at 940 °C for 1 h (a−c) and 6 h (d−f): (a, d) Phase maps; (b, e) IPF maps; (c, f) Pole figures

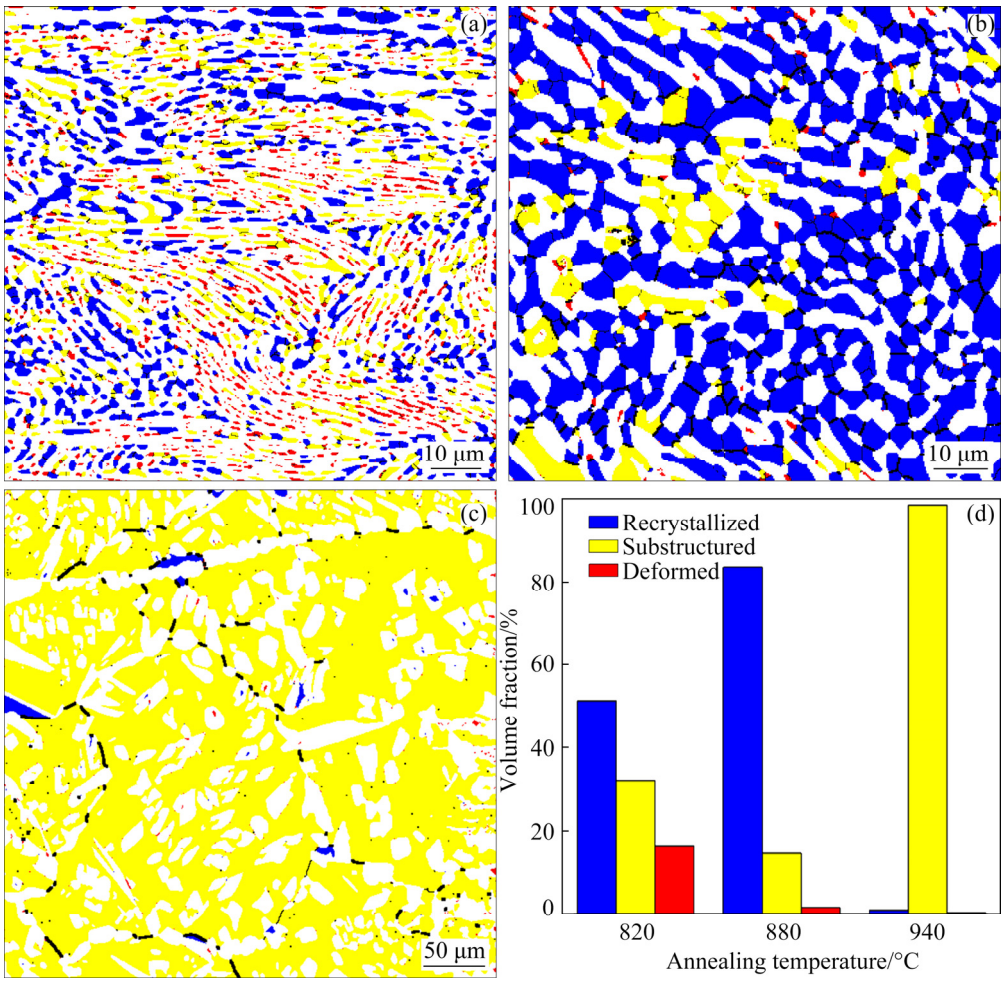

Fig. 11 IAMA maps showing recrystallized, substructured and deformed regions of β phases in annealed microstructures acquired by different annealing processes: (a) 820 °C, 6 h; (b) 880 °C, 6 h; (c) 940 °C, 6 h; (d) Statistics data of volume fraction of recrystallized, substructured and deformed region

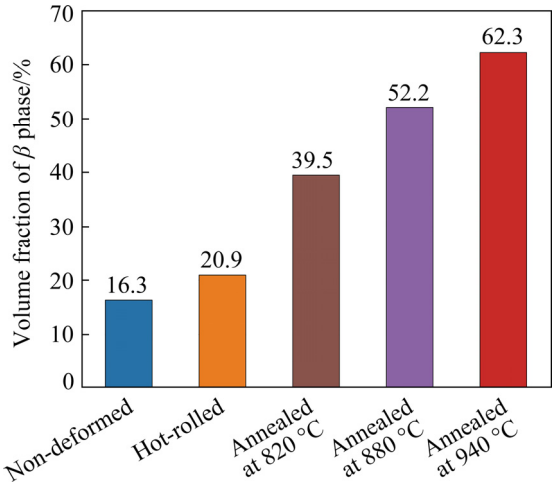

Fig. 12 Volume fraction of β phase in various processing conditions

from rapid phase transformation, would also suppress the formation of LAGBs by SRV in β phase. As a result, the refinement of β grain by SRV and SRX hardly happens during annealing at 940 °C, and α grains distribute inside coarse β grains.

The orientation relationships (ORs) between α and β phases are examined via pole figures in Figs. 10(c, f). Most irregular α grains and some globularized α grains have a nearly Burgers OR with β phase as attested by the coincident $\{0001\}_\alpha // \{110\}_\beta$ planes and $\langle 11\bar{2}0\rangle_\alpha // \langle 111\rangle_\beta$ directions (as pointed out by color arrows in Figs. 10(c, f)), and only a part of globularized α grains deviate from Burgers OR (as marked by ellipse in Figs. 10(c, f)). This can be firstly ascribed to the fact that the lack of SRX in β phase at 940 °C could not change the orientation of β grain apparently. Meanwhile, for the globularized α grains generated by boundary splitting, the combined effect of deformation, SRV and SRX would destroy Burgers OR between α and β phases

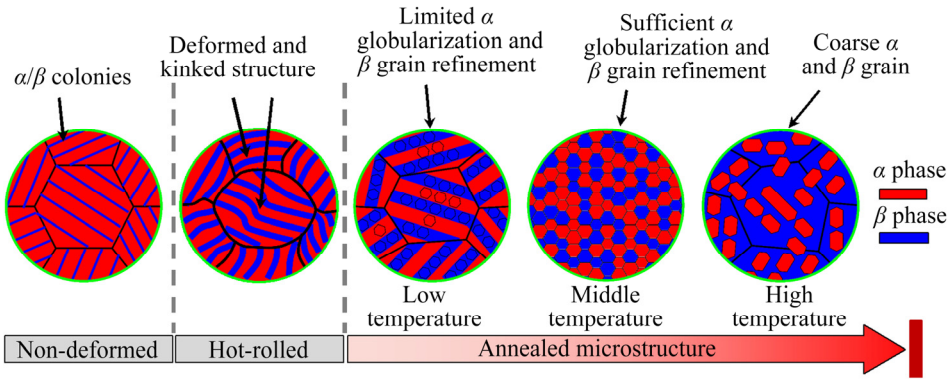

Fig. 13 Schematic illustration conclusively showing globularization and grain morphology evolution of both α and β phases during hot rolling and annealing of TC21 titanium alloy

in the initial colony. However, for the rest of α lamellae, the small deformation amount could not destroy Burgers OR completely, and the subsequent processes of termination migration and Ostwald ripening just change the geometric morphology rather than crystallographic orientation.

Based on the above results, it can be concluded that microstructure evolution of TC21 titanium alloy strongly depends on annealing temperature, as schematically illustrated in Fig. 13. At low annealing temperature (820 °C), boundary splitting acts as the main globularization mechanism for α phase. However, low annealing temperature just leads to limited globularization. As the annealing temperature increases to 880 °C, boundary splitting and termination migration are enhanced, which induces sufficient globularization. Meanwhile, sufficient SRV and SRX promote formation of LAGBs and HAGBs, which in turn refines interlamellar β completely. At excessively high annealing temperature of 940 °C, the α grain coarsening by Ostwald ripening, and the weakened SRV and SRX restrain grain refinement of β phase, resulting in the distribution of α grain in coarse β grains. Accordingly, it is found that intermediate annealing temperature, i.e. 880 °C in this work, is appropriate to get a homogeneous microstructure, in which the globularized α grains and refined β grains are adjacent to each other and homogeneously distributed.

4 Conclusions

(1) The rolling at low temperature of 750 °C suppresses DRV/DRX and globularization of α and β phases during rolling. Most α colonies exhibit lamellar morphology except that a few α lamellae are kinked after rolling.

(2) Low annealing temperature of 820 °C just leads to limited globularization of α lamellae by boundary splitting. Increasing the annealing temperature to 880 °C and prolonging annealing time to 6 h enhance the boundary splitting and termination migration, which result in sufficient globularization of α phase. At the excessively high annealing temperature of 940 °C, Ostwald ripening leads to an apparent α grain coarsening.

(3) SRV and SRX produce LAGBs and HAGBs, which divide interlamellar β into refined β grains. Sufficient β grain refinement is achieved at the annealing temperature of 880 °C. However, the excessively high annealing temperature (940 °C) restrains the formation of LAGBs and HAGBs, which subsequently leads to the coarse β grains.

(4) Intermediate temperature (~880 °C) is appropriate to get a homogeneous microstructure in which the globularized α grains and refined β grains distribute homogeneously.

Acknowledgments

The authors are grateful for the financial supports from the National Natural Science Foundation of China (No. 51971046) and the Fundamental Research Funds for the Central Universities, China (No. 2020CDJGFCL005)

References

[1] FAN R L, WU Y, CHEN M H, XIE L S. Relationship among microstructure, mechanical properties and texture of TA32 titanium alloy sheets during hot tensile deformation [J]. Transactions of Nonferrous Metals Society of China, 2020, 30: 928−943.

[2] NONG Z S, LEI Y N, ZHU J C. Effect of α phase on evolution of oxygen-rich layer on titanium alloys [J]. Transactions of Nonferrous Metals Society of China, 2019, 29: 534−545.

[3] FAN X G, ZENG X, YANG H, GAO P F, MENG M, ZUO R, LEI P H. Deformation banding in β working of two-phase TA15 titanium alloy [J]. Transactions of Nonferrous Metals Society of China, 2017, 27: 2390−2399.

[4] WU M Y, XIN R L, WANG Y, ZHOU Y, WANG K, LIU Q. Microstructure, texture and mechanical properties of commercial high-purity thick titanium plates jointed by electron beam welding [J]. Materials Science and Engineering A, 2016, 677: 50−57.

[5] SHI Z F, GUO H Z, ZHANG J W, YIN J N. Microstructure−fracture toughness relationships and toughening mechanism of TC21 titanium alloy with lamellar microstructure [J]. Transactions of Nonferrous Metals Society of China, 2018, 28: 2440−2448.

[6] MAZURSKI M I, SALISHCHEV G A. Effect of interface energy anisotropy on thermal stability and transformation of lamellar structures. II: Transformation of lamellae [J]. Physica Starus Solidi B − Basic Solid State Physics, 1995, 188: 653−658.

[7] SEMIATIN S L, SEETHARAMAN V, WEISS I. Flow behavior and globularization kinetics during hot working of Ti−6Al−4V with a colony alpha microstructure [J]. Materials Science and Engineering A, 1999, 263: 257−271.

[8] PARK C H, KO Y G, PARK J W, LEE C S. Enhanced superplasticity utilizing dynamic globularization of Ti−6Al−4V alloy [J]. Materials Science and Engineering A, 2008, 496: 150−158.

[9] WANG K X, ZENG W D, ZHAO Y Q, SHAO Y T, ZHOU Y G. Prediction of dynamic globularization of Ti-17 titanium alloy with initial lamellar microstructure during hot compression [J]. Materials Science and Engineering A, 2010, 527: 6193−6199.

[10] WU C B, HE Y, FAN X G, SUN Z C. Dynamic globularization kinetics during hot working of TA15 titanium alloy with colony microstructure [J]. Transactions of Nonferrous Metals Society of China, 2011, 21: 1963−1969.

[11] WANG K X, ZENG W D, ZHAO Y Q, LAI Y J, ZHOU Y G. Dynamic globularization kinetics during hot working of Ti-17 alloy with initial lamellar microstructure [J]. Materials Science and Engineering A, 2010, 527: 2559−2566.

[12] ROY S, SUWAS S. Enhanced superplasticity for (α+β)-hot rolled Ti−6Al−4V−0.1B alloy by means of dynamic globularization [J]. Materials and Design, 2014, 58: 52−64.

[13] STEFANSSON N, SEMIATIN S L, EYLON D. The kinetics of static globularization of Ti−6Al−4V [J]. Metallurgical and Materials Transactions A, 2002, 33: 3527−3534.

[14] STEFANSSON N, SEMIATIN S L. Mechanisms of globularization of Ti−6Al−4V during static heat treatment [J]. Metallurgical and Materials Transactions A, 2003, 34: 691−698.

[15] SEMIATIN S L, KNISLEY S L, FAGIN P N, ZHANG F, BARKER D R. Microstructure evolution during alpha−beta heat treatment of Ti−6Al−4V [J]. Metallurgical and Materials Transactions A, 2003, 34: 2377−2386.

[16] WEISS I, FROES F H, FYLON D, WELSCH G E. Modification of alpha morphology in Ti−6Al−4V by thermomechanical processing [J]. Metallurgical and Materials Transactions A, 1986, 17: 1935−1947.

[17] AHEREBTSOV S, MURZINOVA M, SALISHCHEV G, SEMIATIN S L. Spheroidization of the lamellar microstructure in Ti−6Al−4V alloy during warm deformation and annealing [J]. Acta Materialia, 2011, 59: 4138−4150.

[18] XU J W, ZENG W D, MA H Y, ZHOU D D. Static globularization mechanism of Ti-17 alloy during heat treatment [J]. Journal of Alloys and Compounds, 2018, 736: 99−107.

[19] FAN X G, ZHENG H J, ZHANG Y, ZHANG Z Q, GAO P F, ZHAN M, LIU J. Acceleration of globularization during interrupted compression of a two-phase titanium alloy [J]. Materials Science and Engineering A, 2018, 720: 214−224.

[20] GAO P F, FU M W, ZHAN M, LEI Z N, LI Y X. Deformation behavior and microstructure evolution of titanium alloys with lamellar microstructure in hot working process: A review [J]. Journal of Materials Science & Technology, 2020, 39: 56−73.

[21] SEMIATIN S L. An overview of the thermomechanical processing of α/β titanium alloys: Current status and future research opportunities [J]. Metallurgical and Materials Transactions A, 2020, 51: 2593−2625.

[22] WANG L, FAN X G, ZHAN M, JIANG X Q, ZENG X, LIANG Y F, ZHANG H J, ZHAO A M. The heterogeneous globularization related to crystal and geometrical orientation of two-phase titanium alloys with a colony microstructure [J]. Materials and Design, 2020, 186: 108338.

[23] ROY S, SUWAS S. Microstructure and texture evolution during sub-transus thermomechanical processing of Ti−6Al−4V−0.1B alloy. Part I: Hot rolling in (α+β) phase field [J]. Metallurgical and Materials Transactions A, 2013, 44: 3303−3321.

[24] ROY S, KARANTH S, SUWAS S. Microstructure and texture evolution during sub-transus thermo-mechanical processing of Ti−6Al−4V−0.1B alloy. Part II: Static annealing in (α+β) regime [J]. Metallurgical and Materials Transactions A, 2013, 44: 3322−3336.

[25] ROY S, SUWAS S. Orientation dependent spheroidization response and macro-zone formation during sub β-transus processing of Ti−6Al−4V alloy [J]. Acta Materialia, 2017, 134: 283−301.

[26] TARZIMOGHADAM Z, SANDLOBES S, PRADEEP K G. Microstructure design and mechanical properties in a near-α Ti−4Mo alloy [J]. Acta Materialia, 2015, 97: 291−304.

[27] WANG K, WU M Y, YAN Z B, LI D R, XIN R L, LIU Q. Dynamic restoration and deformation heterogeneity during hot deformation of a duplex-structure TC21 titanium alloy [J]. Materials Science and Engineering A, 2018, 712: 440−452.

[28] MIRONOV S, MURZINOVA M, ZHEREBTSOV S. Microstructure evolution during warm working of Ti−6Al−4V with a colony-α microstructure [J]. Acta Materialia, 2009, 57: 2470−2481.

[29] STEINER M A, MCCZBE R J, GARLEA E. Monte Carlo modeling of recrystallization processes in α-uranium [J]. Journal of Nuclear Materials, 2017, 492: 74−87.

[30] XU J W, SUN X, JIA Z Q, ZHOU J H. Static coarsening

behavior of the lamellar alpha in Ti-17 alloy [J]. Journal of Alloys and Compounds, 2015, 631: 248−254.
[31] SHAHANI A J, XIAO X, SKINNER K, PETERS M, VOORHEES P W. Ostwald ripening of faceted Si particles in an Al−Si−Cu melt [J]. Materials Science and Engineering A, 2016, 673: 307−320.
[32] FAN X G, YANG H, YAN S L, GAO P F, ZHOU J H. Mechanism and kinetics of static globularization in TA15 titanium alloy with transformed structure [J]. Journal of Alloys and Compounds, 2012, 533: 1−8.
[33] STREITENBERGER P, ZOLLNER D. The envelope of size distributions in Ostwald ripening and grain growth [J]. Acta Materialia, 2015, 88: 334−345.
[34] WANG K, WU M Y, YAN Z B, LI D R, XIN R L, LIU Q. Microstructure evolution and static recrystallization during hot rolling and annealing of an equiaxed-structure TC21 titanium alloy [J]. Journal of Alloys and Compounds, 2018, 752: 14−22.
[35] WANG K, LI M Q, LIU Q. Evolution mechanisms of the primary α and β phases during α/β deformation of an α/β titanium alloy TC8 [J]. Materials Characterization, 2016, 120: 115−123.

TC21 钛合金热轧后退火过程中 α 和 β 相静态球化和晶粒形貌演变

王 柯，吴明玉，任 朝，张 宇，辛仁龙，刘 庆

重庆大学 材料科学与工程学院 轻合金材料国际合作联合实验室，重庆 400044

摘 要：对具有片层组织的 TC21 钛合金金进行热轧和退火试验(退火温度：820、880、940 °C；退火时间：1、6 h)，进而研究退火参数对 α 和 β 相静态球化和晶粒形貌的影响。结果表明：退火温度为 820 °C 时，α 球化不明显，这是由于片层 α 相中晶界分离机制受限所致。当退火温度升高到 880 °C 时，晶界分离和末端迁移两种球化机制的发生促进片层 α 相的球化。在 820 和 880 °C 退火时，静态回复和静态再结晶导致片层间 β 晶粒发生细化。然而，过高的退火温度(940 °C)使得 α 晶粒在奥施特瓦尔德熟化作用下发生粗化，同时抑制片层间 β 相中静态再结晶的发生，产生粗大的 β 晶粒。因此，880 °C 是一个合适的退火温度；在该退火温度条件下可获得均匀的退火组织，其中球化的 α 晶粒和细化的 β 晶粒均匀分布。

关键词：TC21 钛合金；α 球化；再结晶；晶粒细化

(Edited by Bing YANG)